

N 113

7/11-7/13 1993

10/11/93

A comparison of gamma-ray and radio emissions during the 11:42 UT solar flare on 1982 June 3

G. Trottet¹, E.L. Chupp², H. Marschhäuser³, M. Pick¹, I. Soru-Escut⁴, E. Rieger³, and P.P. Dunphy²

¹ Observatoire de Paris Section de Meudon, DASOP and CNRS-URA 324, F-92195 Meudon Principal, Cedex, France

² University of New Hampshire Physics Department and Space Science Center, Durham, NH 03824, USA

³ Max-Planck-Institut für Extraterrestrische Physik, Giessenbach-Strasse, D-85740 Garching bei München, Germany

⁴ Observatoire de Paris Section de Meudon, DASOP and CNRS-URA 326, F-92195 Meudon Principal, Cedex, France

Received 28 October 1993 / Accepted 22 December 1993

Abstract. We report new, unpublished data for the X class solar flare on 1982 June 3 at 1142 UT (X8), using data from the *SMM* GRS, the Nançay Radioheliograph, the RSTN network, and two optical observatories. We demonstrate that ion and relativistic electron acceleration both occur before the rise of the initial major photon burst. We have also carried out a detailed comparison of the time histories for emissions at 169 MHz, several microwave frequencies, and X-ray and γ -ray energies from 14 keV to above 10 MeV. The comparisons clearly show: (i) a close time correlation of all emissions during the initial phase of the event, indicating that acceleration (or release) of the electrons and ions responsible for the different emissions likely came from the same source, (ii) the different hard X-ray and γ ray peaks are associated with the appearance of new 169 MHz radio sources. During the later phase of this event the energetic emissions were predominately γ rays and high-energy neutrons resulting from an extended acceleration or trapping plus precipitation phase characterized by energetic ions with energies up to a GeV with little or no evidence for the presence of relativistic electrons. During this time a moving Type IV burst developed and persisted for at least 6 minutes. The Nançay radioheliograph data do not show evidence for a large scale coronal Type II shock. The results presented here show that the magnetic field topology of the acceleration region evolves throughout the event indicating that acceleration in proposed simple single loop models is not viable. From this analysis we conclude that the two bursts of high-energy emissions which characterize this flare are due to two different particle populations, which are accelerated and propagate in different magnetic structures.

Key words: acceleration of particles – Sun: activity, flares, radio radiation, gamma rays

1. Introduction

It is now well established that acceleration of both relativistic electrons and γ -ray line producing ions is a common feature of the so called “impulsive solar flare” (Chupp 1984; Murphy et al. 1992). Indeed there is strong direct evidence that often, if not always, the acceleration of the two particle species is simultaneous, suggesting (in the simplest interpretation), a common acceleration process (Forrest & Chupp 1983; Chupp 1990a). Modelling of some solar flare events now implicitly assumes that a flare is initiated in this manner (Murphy et al. 1987; Kocharov et al. 1988; Guglenko et al. 1990; Ryan & Lee 1991). Even though this new picture of flare particle acceleration is qualitatively and fundamentally different than what was believed before 1980 (Wild et al. 1963; Wild & Smerd 1972), there is no clear understanding as to how particle acceleration is initiated in solar flares or even which mechanisms are applicable in specific cases. For example, a recent paper on prompt ion acceleration in solar flares (Ohsawa 1993) did not even address electron acceleration while the two species may be closely related!

By using hard X-ray spectral and radio imaging observations Raoult et al. (1985) have deduced that changes in the accelerated electron spectrum are directly related to the evolving morphology of the active region magnetic field structure as implied by radioheliograph observations. This general picture was also confirmed by a study of an impulsive flare and a long-term event by Trottet et al. (1993). Recently, Chupp et al. (1993) have carried out a similar study, using multiwavelength observations of a flare that occurred at 09:09 UT on 1989 September 9, which included γ -ray line observations that give direct information on the accelerated ion properties. The results of this study demonstrate that changes in the spectra of both accelerated electrons and ions are associated with the appearance of new coronal radio sources and chromospheric H α sources that are probably connected with the original and new energy release sites. Thus the close connection of ion and electron acceleration and its association with the evolving morphology of the active region

magnetic field is further demonstrated. It is, therefore, of interest to extend such multiwavelength studies to as many other flares for which radio, optical, X- and γ -ray observations exist. In this paper a study is made of new, unreported radio, H α and γ -ray observations for the unusual and dramatic flare at 11:42 UT on 1982 June 3. The new observations, combined with previous analyses of this event give a more complete understanding of ion and electron acceleration. The main goals in this paper are: (i) to determine, as accurately as possible, the onset time of the first nuclear reactions which will demonstrate the presence of energetic ions (~ 30 MeV) and compare with the onset of electron acceleration; (ii) to investigate the morphology of the active region magnetic field for the two bursts which characterize the 1982 June 3 flare.

2. Description of instrumentation

The high-energy photon observations of the flare were made with the Solar Maximum Mission (*SMM*) Gamma-Ray Spectrometer (GRS), and its auxiliary X-ray detectors. The GRS provides flare spectra and background spectra in several energy channels between 14 keV and > 100 MeV with time resolutions ranging from 1.024 s to 16.384 s. A full description of the *SMM* GRS may be found in Forrest et al. (1980).

The radio observations of the flare were made with the Nançay Radioheliograph (NRH) (The Radioheliograph Group 1983). This instrument provides one dimensional images with circular polarization measurements in the east-west (EW) and south-north (SN) directions. In 1982 the Mark III instrument observed only at 169 MHz with a time resolution of 0.04 s. The EW and SN images allow us to obtain the 2-dimensional position of the centroids of the 169 MHz emitting sources projected on the plane of the sky. The spatial resolution is about $1.2'$ and $3.0'$ for the EW and SN arrays, respectively.

For dynamic meterwave spectra, observations were provided by the *ARTEMIS* Radiospectrograph of the Paris Observatory (Department of Space Research, courtesy of J. L. Bougeret and M. Poquerusse) located at Nançay, with 115 channels covering the frequency range from 150 MHz to 470 MHz (Dumas et al. 1982) and at Weißenau from 36 MHz to 1000 MHz (Urbazr 1993).

Additional meterwave and microwave intensity data at several discrete frequencies were provided by the United States Air Force RSTN Station at Sagamore Hill, Massachusetts, USA (courtesy of E. Cliver).

3. Observations

The 1982 June 3 H α 2B (*GOES* X8) white light flare erupted at 11:41 UT (*GOES* 1–8 Å), in NOAA region 3763 (09°S, 71°E), which had produced numerous M- and X-class events between June 2 and 15. Intense electromagnetic emissions were observed from radio to γ -ray wavelengths, followed by a burst of high-energy neutrons observable at the Earth. Intense solar energetic particle emissions (SEP) were recorded first by the *Helios 1*

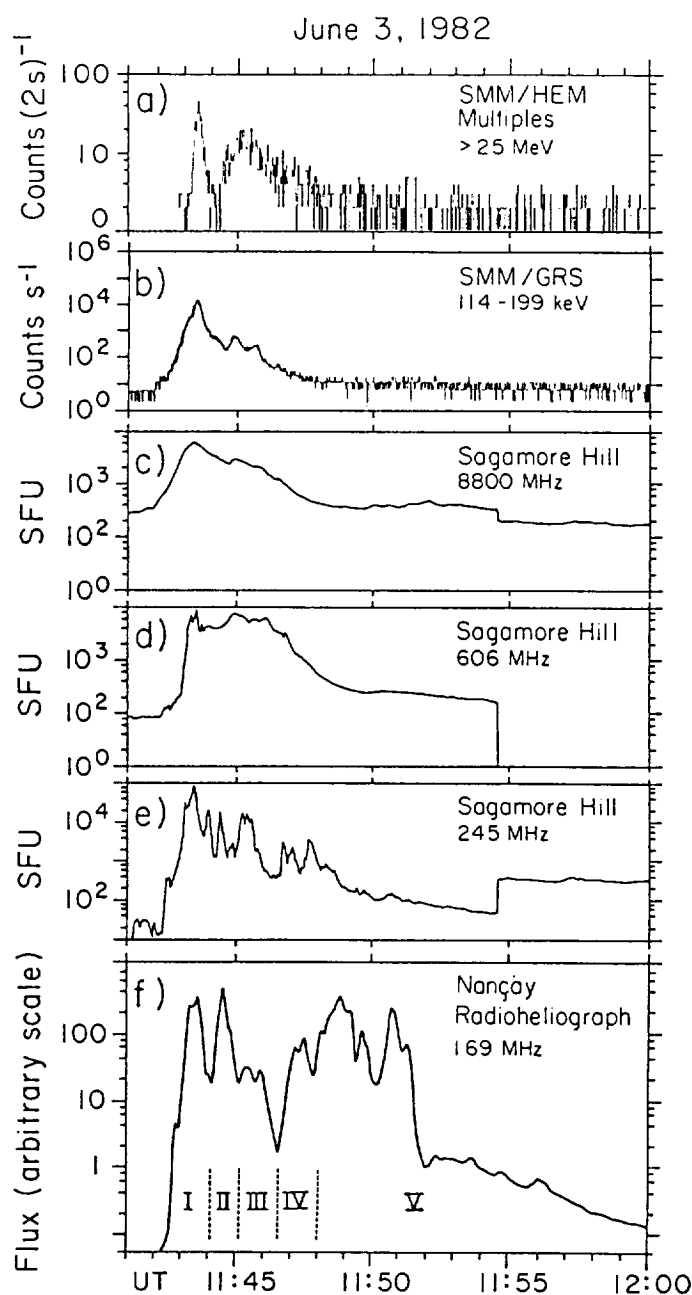


Fig. 1a–f. Time histories, at the highest time resolution, are shown for hard X rays (> 114 keV), γ rays (> 25 MeV), several RSTN radio frequencies (Sagamore Hill) and the 169 MHz Nançay Radioheliograph frequency. Time intervals, when important features occur, are identified by Roman numerals and discussed in Sect. 3

spacecraft at 0.5 AU east of the Earth-Sun line which was well connected to the flaring region. The time history of the γ -ray and X-ray and high-energy neutron emission reported previously by Chupp et al. (1987, 1990a) shows continuous emission over the entire interval from $\sim 11:43$ to 12:04 UT when *SMM* entered into eclipse. Figure 1 (panels a and b) shows the time histories for hard X rays > 114 keV and γ rays > 25 MeV.

In the earlier work a first impulsive burst was identified between $\sim 11:43$ UT and 11:44 UT during which the majority

Table 1. Synopsis of electromagnetic emissions

Time Interval	11:40:32–11:42:20	11:42:20–11:44	11:44–11:48	After 11:48
	Event Initiation	First Burst	Extended emission	
SXR	GOES, HXRBS, GRS			
HXR	100 keV 11:42:00			
γ R (> 300 keV)	no emission	11:42:40		
γ R lines	no emission	11:42:27		
GRS (> 10 MeV)	no emission	11:42:50		
NRH	no emission	A 11:42:20 (I) A' 11:43	B-B' 11:44–11:45 (II) C-C' 11:45–11:46:30 (III) D 11:46:30–11:48 (IV)	moving Type IV Source D moves Northward (V)
Radio Spectral Characteristics	Microwave 11:43:30	U, J, III, V continuum dam- λ -cm- λ after 11:43	dam-cm continuum slow drifting features in dm-m range	m-dam continuum drifting slowly toward low frequencies

Note: The time indicated for γ R lines (i.e. 11:42:27) is the beginning of a 16.384 s *SMM* GRS accumulation interval which ends at 11:42:43.5 UT. Therefore, a precise initiation time of γ -ray line emission in this interval cannot be determined.

of the total emission for all energies < 25 MeV is produced. During this period, Forrest et al. (1985), have also demonstrated the presence of electron bremsstrahlung to, at least, 40 MeV and π^0 meson decay γ rays extending in energy above 100 MeV. A second burst starting around 11:44 UT, initiated an extended phase during which most of the γ -ray emission is produced by pion decay γ rays. Forrest et al. (1985), have shown that 80% of the meson decay photons were produced in the extended phase of the event which also gave rise to an intense flux of neutrons observable at the Earth (Chupp et al. 1987). A complete review of the emission characteristics of this event has been given by Chupp (1990b), based on published works to mid-1989. In the following we present a detailed comparison of the GRS observations, the radio observations obtained at 169 MHz with the NRH and with radio spectral data obtained by the *ARTEMIS* radiospectrograph at Nançay in the (150–470) MHz band and at Weißenau in the (36–1000) MHz domain. Figure 1 (panels c–f) shows the time evolution of the event at several microwave frequencies and at 169 MHz, the single operating frequency of the NRH.

The evolution of the radio emission at 169 MHz observed during the full event is displayed in Fig. 2, which shows isointensity contours as a function of time. The figure indicates that the emission arises from different sources (marked by capital letters) which appear at different times as the event evolves. In accordance with the time profile of the > 25 MeV emission, shown in Fig. 1 (panel a) and the evolution of the 169 MHz radio emission pattern shown in Fig. 2, we divide the event into five time intervals in each of which distinctive features appear. These intervals, shown in Figs. 1 and 4, indicate the time of appearance and duration of X-ray, γ -ray line, and continuum (> 10 MeV) emissions, as well as the intervals of time during which given radio sources are observed. Table 1 summarizes all the electromagnetic emissions and gives the spectral characteristics of the radio emission. The NRH row in the table defines the precise times of these intervals in roman numerals and should not be confused with spectral types.

3.1. Event initiation: 11:40:32–11:42:20 UT

The *SMM* HXRBS reports a start time for the 1982 June 3 event at 11:40:32 UT (Dennis et al. 1991) for X rays > 25 keV. Using the HXRBS and ISEE-3 data, Klein et al. (1987) have found that the onset of X-ray emission occurs progressively later, the higher the photon energy. This fact is confirmed by the *SMM* GRS auxiliary X-ray detectors. During the interval of time considered here only photon energies below 150 keV were observed. In the radio domain weak microwave emission is observed and only a weak fast drift burst is detected at 11:42:13 UT in the decimeter to meterwave bands.

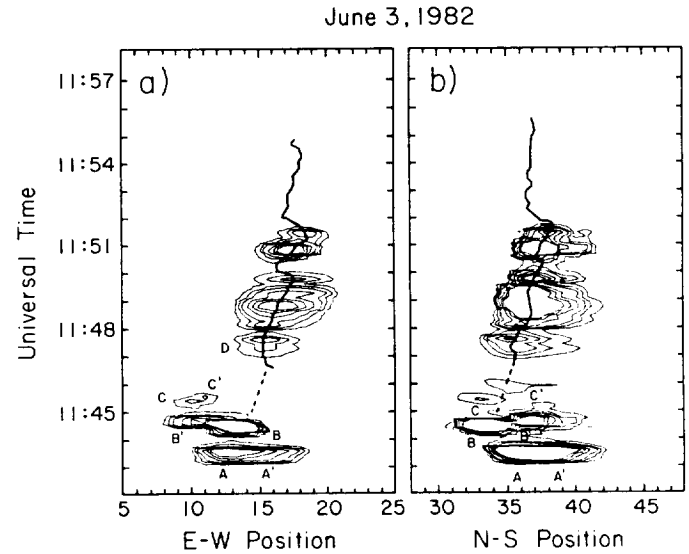


Fig. 2a and b. The Nançay radioheliograph isointensity contours for the east-west (a) and north-south arrays (b) show the meterwave sources at 169 MHz as a function of time during the 1982 June 3 flare. The solid lines indicate the east-west and north-south positions of the 169 MHz source after 11:47 UT. The positions are given in instrumental units (1 unit corresponds to about 0.07 and 0.12 solar radii in the east-west and north-south directions, respectively). The center of the Sun is at 33 in both directions

3.2. First burst 11:42:20–11:44:00 UT

Figure 1 shows that the first major hard X-ray > 114 keV and γ -ray > 25 MeV bursts are initiated slightly before 11:42:50 UT and reach maxima around 11:43:30 UT. Since it is of particular interest to determine when ion acceleration is first evident we study the evolution of the γ -ray emission during the initial rising phase of the first burst starting at 11:42:27.2 UT until 11:42:59.9 UT. The two photon-spectra for this time interval (temporal resolution 16.384 s) are shown in Fig. 3. They were obtained by a direct deconvolution of the background-subtracted GRS count spectra (Marschhäuser et al. 1992; Marschhäuser 1993) using the UNH GRS response function model (Vers. 3.1) (Forrest 1992).

For both spectra, due to poor statistics, a quantitative separation of γ -ray line emission, produced by nuclear reactions, and continuum emission from bremsstrahlung of energetic electrons, is not possible. Usually, the dominant bremsstrahlung continuum below 1 MeV can be well approximated in flare γ -ray spectra by simple power laws. However, in the first spectrum (11:42:27.2–11:42:43.5) UT the best powerlaw fit to the data < 1 MeV, as indicated in Fig. 3 (panel a) and given by $(7.5 \times (E/1\text{ MeV})^{-2.93 \pm 0.2})$, is only poorly defined. An extrapolation of this power law to higher energies exceeds the observed low flux between 1 and 3 MeV as shown in Fig. 3 (panel a). We therefore conclude that the true bremsstrahlung continuum is substantially steeper and deviates from a simple power-law behavior above ~ 1 MeV! This initial spectrum, although less intense than the following spectrum at 11:42:43.5–11:42:59.9 UT, and shown in Fig. 3 (panel b), reveals over the whole energy range from 0.3 MeV to 9 MeV the typical signature of nuclear components in flare γ -ray spectra. Even when taking the extrapolated power law as an upper limit for the flux due to bremsstrahlung, the significant excess above this line of reference at energies > 3 MeV can be identified as unresolved and/or kinematically broadened nuclear lines. Furthermore, the two line features at 1.4 MeV and 1.6 MeV are in agreement with the strong deexcitation lines from Mg and Ne, respectively (see Ramaty et al. 1979). This observation clearly shows that γ -ray line producing ions (~ 30 MeV protons) have been produced early in the 1982 June 3 flare along with high-energy electrons (Lorentz factor $\gamma \gtrsim 1.6$), before the major burst which began at about 11:42:50 UT.

In the second spectrum (11:42:43.5–11:42:59.9) in Fig. 3 (panel b) the intense bremsstrahlung dominates over the entire energy range. The equation of the power-law fit shown in the figure is given by $(70 \pm 2.2) \times (E/1\text{ MeV})^{2.84 \pm 0.08}$. Due to the low line-continuum ratio no significant individual nuclear lines can be identified, but a nuclear line excess is still evident consistent with the fact that nuclear line production started in the previous time interval. According to the above interpretation of the initial spectrum, Fig. 3 (panel a), the bremsstrahlung spectrum is clearly extended above 1 MeV within this succeeding 16 s time interval (Fig. 3, panel b). This is consistent with the earlier analysis of the hard X-ray spectral evolution in this event

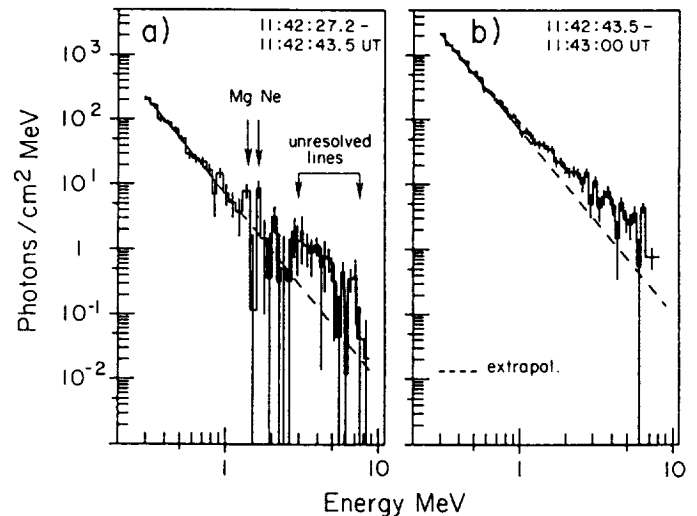


Fig. 3a and b. The deconvolved γ -ray spectra from the *SMM* GRS are shown during the initial part of the 1982 June 3 event. **a** (11:42:27.2–11:42:43.5) UT before the major emission. **b** (11:42:43.5–11:43:00) UT also before the major emission. Both the Mg and Ne lines evident in the **a** spectrum are masked by the greatly increased intense bremsstrahlung shown in the **b** spectrum

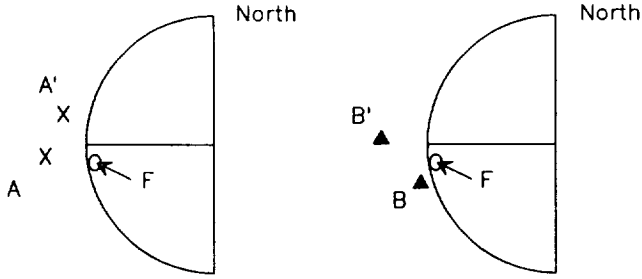
by Klein et al. (1987) which showed a significant flattening at $\sim 11:42:40$ UT.¹

Rieger (1994) has also studied the early development of this event and identified two short bursts of (10–25 MeV) photon emission lasting ~ 5 s at $\sim 11:42:55$ UT and at $\sim 11:43:06$ UT just before the rapid increase of the emission at all energies starting at $\sim 11:43:12$ UT. These peaks which are clearly seen at energies above ~ 300 keV and are hardly recognized at lower energies have been interpreted by Rieger (1994) as a signature of impulsive events with hard electron spectra; i.e., the electron dominated events (Rieger & Marschhäuser 1990) which are superposed on the developing flare emissions. This curious phenomenon is apparently a reflection of chaotic acceleration bursts rather than a process which steadily increases the energy and number of particles.

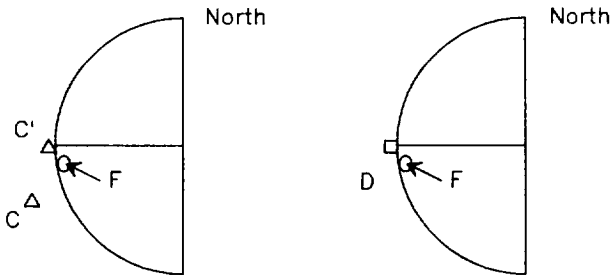
The first significant emission observed at 169 MHz by the NRH is initiated at 11:42:20 UT, arising from a source marked A on Fig. 2. A second source marked A' on Fig. 2 appears at about 11:42:50 UT at a new location. The positions of these two sources are shown in Fig. 4 as projected on the sky in heliographic coordinates. In Fig. 5 the time evolution of A and A' (panel a) is compared with that of the hard X-ray emission (56–199) keV (panel b). This figure shows that the radio and hard X-ray emissions have similar durations. Figure 5 also shows that A and A' (panel a) have comparable intensities after 11:43:06 UT, nearly in coincidence with the start of the fast rise of the (> 25) MeV emission shown in Fig. 1 (panel a). Moreover, A and A' have similar time profiles thereafter indicating that they

¹ Unfortunately, pulse pile-up effects caused by high counting rates do not allow an interpretation of the GRS γ -ray spectra later than 11:43:00 UT

I: 11:42:20 – 11:44:00 UT II: 11:44:00 – 11:45:00 UT



III: 11:45:00 – 11:46:30 UT IV: 11:46:30 – 11:48:00 UT



V: after 11:48:00 UT

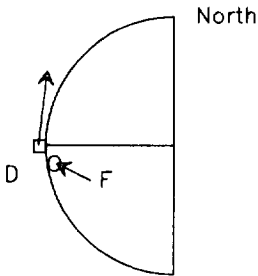


Fig. 4. The location of the 169 MHz sources for the five intervals of time marked I, II, III, IV and V on Fig. 1 (see also Table 1). The flare region (F) is indicated by an open circle

both are fed by a common injection of electrons into different large scale magnetic structures extending into the corona.

The dynamic spectrum for the (150–470) MHz frequency band, shown in Fig. 6 indicates that the emission consists of a series of fast drift bursts (III,U,J) starting at 11:42:19 UT around 200 MHz. The starting frequencies of these bursts drift to higher values and a Type V continuum becomes visible at 11:42:52 UT. The emissions then extend rapidly to higher frequencies and cover the whole (150–470) MHz band by 11:43:00 UT. Dynamic spectra from Weißenau and single frequency records in the microwave domain indicate that, at that time, radio emission is detected in the whole radio spectrum from dekameter to centimeter wavelengths.

The appearance of a new radio source at meter wavelengths and the spread of the low frequency radio emission to decimeter wavelengths, which are observed during the rising part of

June 3, 1982

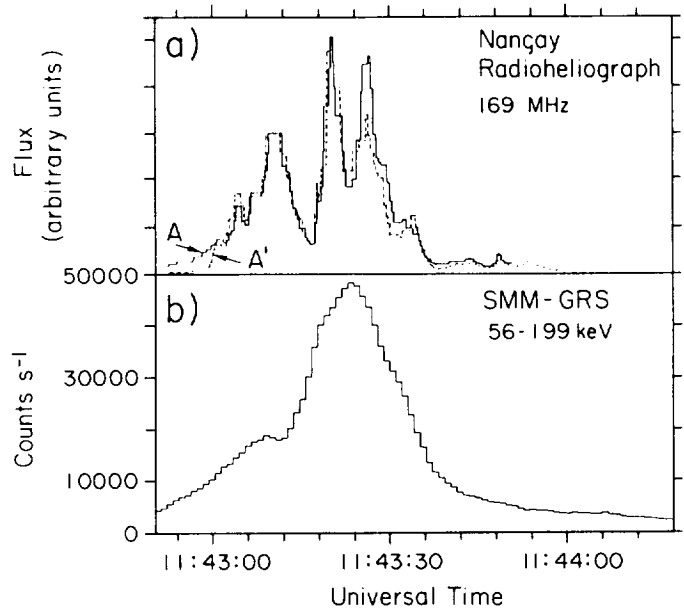


Fig. 5a and b. The time history of hard X rays (56–199) keV and the 169 MHz radio emissions are compared, indicating that both emissions are of comparable duration. Also, the sources A and A' (see Fig. 2) have similar time profiles after 11:43:06 UT

the first major burst during the 1982 June 3 event, is a typical signature of the buildup of impulsive flares (e.g., Raoult et al. 1985).

3.3. Second burst 11:44–11:48 UT

Figure 1 shows that the second burst is characterized by two peaks (at $\sim 11:44:40$ and $11:45:40$ UT) in the (114–199) keV band and by a broad peak (at $\sim 11:45$ UT) in the (> 25) MeV band. (After 11:48 UT the hard X-ray and the microwave emission intensities do not show structure in their time evolution and slowly decay; see below.)

Figure 2 shows that the 169 MHz emission observed between 11:44 and 11:48 UT originates from a complex of sources which are at other locations than the sources A and A' detected during the first burst. This new emission originates from sources marked B and B' as shown in Fig. 2 which appear between 11:44 and 11:45 UT in association with a subpeak in the hard X rays (see Fig. 1). Another pair of radio sources, C and C', appears in association with another hard X-ray subpeak between 11:45 and 11:46:30 UT. An additional radio source, D, appears between 11:46:30 and 11:48 UT. It is associated with a peak in the 8800 MHz time profile which may also be present in the (114–199) keV time history (see Fig. 1 panel b). The projected positions of the radio sources B–B', C–C' and D are shown in Fig. 4.

The dynamic spectrum shown in Fig. 6 indicates that the shift of the 169 MHz emission from sources A–A' to the sources B–B', C–C' and D correspond to changes of the spectral characteristics of the radio emission. Indeed, during the time inter-

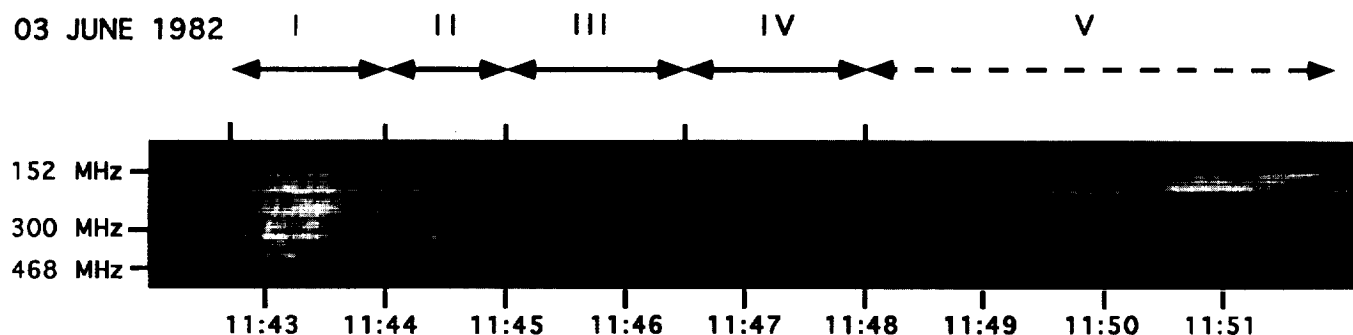


Fig. 6. Radio dynamic spectrum in the (150–470) MHz frequency band observed during the 1982 June 3 flare with the *ARTEMIS* radiospectrograph of Paris Observatory (Department of Space Research) located at Nançay (courtesy of J.L. Bougeret and M. Poquerusse). The five intervals of time defined in Figs. 1 and 4 are reported on the upper abscissa axis

vals marked II, III and IV on the figure, one sees slow drifting ($\sim 5 \text{ MHz s}^{-1}$) narrow band emission features superposed on a wide band continuum.

3.4. Extended emission >11:48 UT

After 11:48 UT, the hard X-ray and γ -ray line emissions have decayed to near background levels while the GRS energy-loss rates above 25 MeV remain at nearly the same level for several minutes (see Chupp et al. 1987; Chupp 1990b). This characteristic of the 1982 June 3 high-energy flare emissions has been explained as a combination of meson decay γ rays (Forrest et al. 1985) and the arrival of high-energy neutrons (Chupp et al. 1987) at the spacecraft, however, Fig. 1 (panel a) only shows the γ -ray time history. The microwave emission is also smoothly decaying as shown in Fig. 1 (panels c and d). In Fig. 6 (interval V) it is evident that the meterwave radio emission is restricted to frequencies below $\sim 200 \text{ MHz}$ and consists of a wide band continuum, the starting frequency drifting slowly towards low frequencies. Such a pattern is usually typical of Type II shock emission. However, as shown in Fig. 2, at 169 MHz the emission arises from a moving source which travels northward (see also Fig. 4, panel V) with a projected velocity of $\sim 400 \text{ km s}^{-1}$. Thus, according to the 169 MHz NRH observations, the radio emission after 11:48 UT is most likely from a moving Type IV continuum source rather than from a Type II burst which would result from a moving disturbance which, at a given frequency, would have been detected as a source at a fixed position.

3.5. $H\alpha$ emission

Unfortunately the $H\alpha$ observations of this flare are sparse being limited to filtergram observations at 11:40 and 11:41 UT at the beginning of the flare and at 11:45 UT during the second emission period as discussed above. Figure 7 shows photographs obtained from Catania (upper panel, courtesy of Dr. Rodono) and Kanzelhöhe (lower panel, courtesy of Dr. Otruba). In spite of this meager information, it is interesting to note that both observatories record the presence of a bright $H\alpha$ region at 11:45 UT several degrees north of the active region in which the first

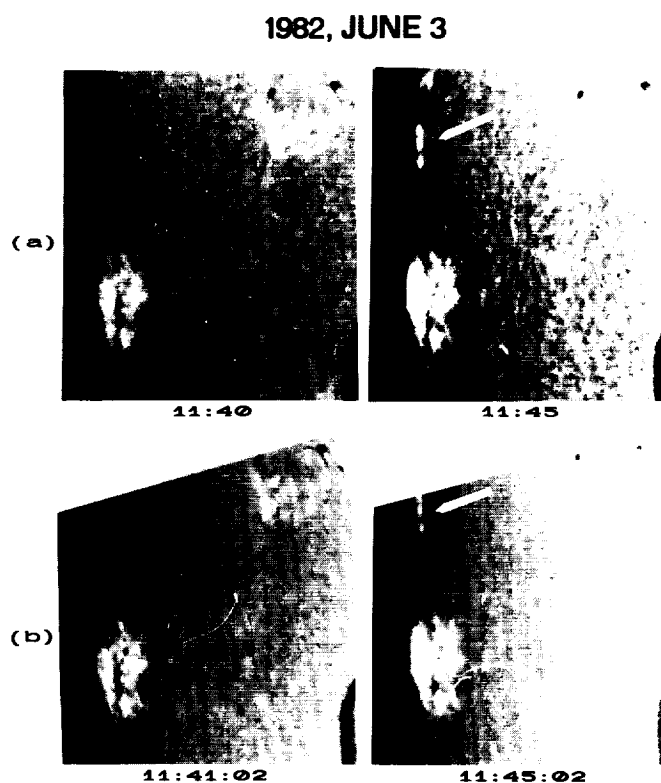


Fig. 7a and b. The 1982 June 3 flare observed at two times in $H\alpha$ (a) at Catania (courtesy of Dr. Rodono) and at similar times (b) at Kanzelhöhe (courtesy of Dr. Otruba)

brightening occurred. It is not possible to know when this feature was initiated but the later appearance of additional $H\alpha$ emission regions remote from the primary flare is relatively common (Wülser et al. 1990) for flares giving rise to high energy γ rays. This was also the case for the 1989 September 9 flare (Chupp et al. 1993).

4. Discussion

The evidence for early ion acceleration based on γ -ray observations, and the association of changes in the photon spectrum

with the time of appearance of new radio sources are presented here for the first time for this event. The latter has been observed however for other flares (Raoult et al. 1985; Trottet 1986; Trottet et al. 1993; Willson et al. 1990; Chupp et al. 1993). Because of the impulsive nature of the spectral changes and the location of the different coronal sources it is clear that the evolution of this flare involves successively different regions that are probably connected magnetically. The picture that an impulsive flare from its very beginning involves processes occurring within a single region (e.g., a single loop) cannot be used to explain the development of this flare. The growing efficiency of the production of accelerated ions and electrons as reflected in the increasing yield of high-energy photons in the beginning of this event can be interpreted most simply as the energization of the particles in regions where the magnetic field topology increases in complexity. It is important to note the additional early appearance of sporadic bursts of relativistic electrons ($\gamma > 20$) in this event (Rieger 1994).

We have observed that the radio spectrum has different characteristics as the flare evolves. The radio emissions in the first burst are Type III, J and V while during the extended emission between 11:44 UT and 11:48 UT it consists primarily of a wide band continuum and features of narrower bandwidth drifting from high to low frequencies. If the drifting features are associated with an upward moving coronal disturbance then using a standard scale height value we obtain a velocity of 2000–3000 km s⁻¹. While this is typical of shock velocities there is no NRH evidence for a large scale Type II coronal shock. Indeed, the slow drifting continuum observed after 11:48 UT (see Figs. 2, 4, and 6) is due to a northward moving Type IV burst with a velocity of ~ 400 km s⁻¹.

The previous studies of this event have concentrated on quantifying and interpreting the γ -ray line, high-energy γ -ray and neutron emissions from this event.² This was the first event in which both meson-decay γ rays were detected by the *SMM* GRS (Forrest et al. 1985) and high energy neutrons were detected at ground level by Debrunner et al. (1984). These results have been extensively discussed by Chupp (1984), Chupp et al. (1987), Chupp (1990b) and theoretical modeling of the high-energy emissions has been carried out by Ramaty and collaborators (Murphy et al. 1987; Ramaty et al. 1990) and Kocharov and collaborators (Kocharov et al. 1988; Guglenko et al. 1990). The former authors have argued that the emissions in the first and second bursts are due to two different populations of particles. Their analysis assumes that the first group of particles is accelerated by a stochastic process, presumably in a closed magnetic loop, and the second by a diffusive shock in the corona. The stochastic and shock particle spectra are described respectively, by a Bessel function with $\alpha T = 0.04$ and a form $p^{-s} \times \exp(-E/E_{\text{op}})$ where p , E and E_{op} are in turn the particle momentum, energy and turn-over kinetic energy. To fit the γ -ray and neutron observations the number of stochastic particles is $N_p(> 30 \text{ MeV}) = 3.5 \times 10^{33}$ and the corresponding number of

shock particles is 2×10^{31} with $s = 2.4$ and $E_{\text{op}} = 300$ MeV. On the other hand the interplanetary proton spectrum observed in space by *Helios 1* (McDonald & Van Hollebeke 1985) is fit by a shock spectrum with $N_p(> 30 \text{ MeV}) = 3 \times 10^{32}$ for $s = 2.4$ and $E_{\text{op}} = 300$ MeV. If it is assumed that the shock environment is on open magnetic field line then the larger fraction of interplanetary to interacting particles is understandable if the same shock process accelerates both species in the same region of space; and only about 10% of the accelerated particles precipitate. There is however no direct proof that this is, in fact, the case and it is equally valid to assume that the two species are accelerated by two separate processes but both triggered by the flare. The absence of direct evidence for a coronal shock strongly suggests that the interplanetary particles (SEP) are accelerated by some other process! However, the new data we have presented here do not contradict the model of Murphy et al. (1987) that the first and extended high-energy γ -ray/neutron emission periods are due to two different acceleration processes, although the first particles need not be accelerated by a stochastic mechanism. The assumption by Murphy et al. (1987) that shocks are responsible for the extended emission is supported by the fact that the radio data suggests the presence of multiple shocks in a limited altitude range in the low and middle corona. Nevertheless the present observations do not provide clues to decide whether the SEP, observed by *Helios*, escape from the multiple shock region or if they are produced by a third process.

Alternately, Kocharov et al. (1988) assumed that particle acceleration took place in a large coronal loop only during the first burst with the second maximum in the high-energy emissions resulting from a sudden rise in MHD turbulence in the loop causing a greatly increased rate of pitch angle scattering and precipitation of GeV protons yielding the time extended meson decay γ rays and neutron emission.³ Using for the primary accelerated particle spectrum a power law with exponent -3.4 and $N_p(> 30 \text{ MeV}) = 2 \times 10^{33}$, Guglenko et al. (1990) were able to fit all observed low and high-energy γ rays and neutrons observed during the event.

Another single flux tube model has been considered by Ryan & Lee (1991) who assume that particles accelerated instantly during the first burst (by an unspecified process) undergo “prolonged and gradual acceleration” to produce the delay between the first and second burst. The gradual acceleration is a result of second order Fermi acceleration in a turbulent MHD wavefield within a loop.

Even though these simple models can explain many of the observed features of the flare, it is difficult to reconcile a single flux tube model with the NRH observations, discussed above, which clearly indicate that the large scale magnetic structure is different during the two bursts and is evolving in a complex way throughout the event.

Mandzhavidze & Ramaty (1992) although assuming a single loop model for analyzing the high-energy emissions from this

² A detailed determination of the γ -ray line spectrum at the peak of this event is not possible because of gain shift of the *SMM* GRS.

³ As pointed out by Ramaty et al. (1990) in discussing this model, the 4–7 MeV and pion γ rays observed in the first burst would be due to the initial isotropically accelerated protons which are in the loss cone.

flare point out that the second major γ -ray emission pulse could be produced by particles trapped in a different loop or even by particles accelerated outside the loop by a coronal shock. Because the NRH data shows no evidence for a meterwave Type II event our radio data do not provide an argument in favor of this latter possibility.

5. Conclusion

The main conclusions from the analysis presented in this paper are:

1. Both ion (~ 30 MeV) and relativistic electron acceleration occur early in this event, about 1 minute before the initiation of the major burst of energetic photons at all energies. This feature is similar to that seen in the 1989 September 9 solar flare recently reported by Chupp et al. (1993).

2. The increased efficiency of the particle production, starting with the onset of the first burst at 11:42:20 UT, is nearly coincident in time with the appearance of a new radio emitting source in the corona. This feature of an impulsive hard X-ray flare has been reported previously by Raoult et al. (1985) and Willson et al. (1990) (cf. also Willson 1993) and is also clearly evident in a significant γ -ray line flare (Chupp et al. 1993). A similar phenomenon has also been detected on ~ 30 keV X-ray images (Hernandez et al. 1986; Machado et al. 1988). This reflects rapid changes in the topology of the flare associated magnetic field driven, for example, by the emergence of new magnetic fluxes and/or by enhanced foot point motion or magnetic shears (e.g., reviews by Hagyard 1990; Martin 1990; Moore 1990 and references therein).

3. The energetic photon and radio emissions, though they arise from sources at very distant locations, switch on and off nearly simultaneously. This indicates that both kinds of emissions, at a given time, are produced by particles which have been drawn from the same region (e.g., Klein et al. 1983; Raoult et al. 1985; Trottet 1986). However, the acceleration mechanism(s) for ions, whether they are different than for electrons or not, operate in different magnetic topologies for the first and second bursts!

4. There is no evidence for a large scale coronal shock from the NRH observations.

In summary we emphasize that the NRH observations show that the large scale magnetic structure evolves in a complicated manner as the event progresses, demonstrating that a simple single loop model is not viable! Our analysis of the 1982 June 3 flare is consistent with the concept of Murphy et al. 1987 that the first and second bursts of energetic photon emissions are due to different particle accelerations. It is also consistent with the same acceleration processes acting in different magnetic environments during the two bursts. While there is no radio signature of shocks during the flash phase our data strongly suggest the presence of shocks during the extended phase. Nevertheless, these shocks are multiple and occur in a limited altitude range in the low and middle corona. Moreover, due to the various

locations of the radio sources it seems unlikely that particle acceleration during the flash phase may serve as a seed population for shock acceleration during the extended phase.

Acknowledgements. One of us (ELC) wishes to acknowledge the support of Centre National de la Recherche Scientifique (CNRS), the Paris Meudon Observatory, the Alexander von Humboldt Foundation and a NATO Collaborative Research Fellowship which made this work possible. The use of the facilities and the hospitality of the CNRS-URA 324 Laboratory (Radioheliograph Group) and of the Max-Planck-Institut für Extraterrestrische Physik, under Drs. Gerhardt Haerendel and Joachim Trümper, is greatly appreciated. We appreciate the use of radio data provided by J.L. Bougeret (Paris Observatory), E. Cliver (Phillips Laboratory), M. Poquerusse (Paris Observatory) and H. Urbarz (Weissenau) and the $H\alpha$ images provided by Dr. Rodono (Catania) and Dr. Otruba (Kanzelhöhe). The work of M.P. and G.T. was supported by Centre National d'Etudes Spatiales. The work at UNH was supported by NASA Grant NAGW-3512. We also appreciate the contribution of Mary M. Chupp in the analysis of the *SMM* GRS data and in the preparation of this manuscript.

References

- Chupp E.L., 1984, *ARA&A* 22, 359
- Chupp E.L., 1987, *Physica Scripta* T18, 5
- Chupp E.L., 1990a, *Sci* 250, 229
- Chupp E.L., 1990b, *ApJS* 73, 213
- Chupp E.L., Debrunner H., Flückiger E., et al., 1987, *ApJ* 318, 913
- Chupp E.L., Trottet G., Marschhäuser H., et al., 1993, *A&A* 275, 602
- Debrunner H., Flückiger E., Chupp E.L., Forrest D.J., 1983, *Proceedings of the 18th Int. Cosmic Ray Conf.* 4, 75
- Dennis B.R., Orwig L.E., Kennard G.S., et al., 1991, *NASA Technical Memorandum* 4332, 101
- Dumas, Caroubalos, Bourget, The Radiospectrograph of the Paris Observatory, The Nancay Radioheliograph (The Radioheliograph Group 1983 report)
- Forrest D.J., 1992, personal communication to H. Marschhäuser
- Forrest D.J., Chupp E.L., Ryan J.M., et al., 1980, *Solar Physics* 65, 15
- Forrest D.J., Chupp E.L., 1983, *Nat* 305, 291
- Forrest D.J., Vestrand W.T., Chupp E.L., et al., 1985, *Proc. 19th Int. Cosmic Ray Conf. (LaJolla)* 4, 146
- ibid 1986, *Adv. Space Phys.* 6 (Oxford: Pergamon) p. 21
- Guglenko V.G., Efimov E., Kocharov G.E., et al., 1990, *ApJS* 73, 227
- Hagyard M.J., 1990, *Journal of Italian Astron. Soc.*, ed. G. Poletto 61, 337
- Hernandez A.M., Machado M.E., Vilmer N., et al., 1986, *A&A* 167, 77
- Klein K.-L., Pick M., Magun A., Dennis, B.R., 1983, *Solar Physics* 84, 295
- Klein K.L., Pick M., Magun A., et al., 1987, *Solar Physics* 111, 225
- Kocharov G.E., 1988, *Leningrad: Ioffe Physical Technical Inst. Report*, No. I-258
- McDonald F.B., Van Hollebeke, M.A.I., 1985, *ApJ* 290, L67
- Machado M.E., Moore R.L., Hernandez A.M., et al., 1988, *ApJ* 326, 425
- Mandzhavidzhe N., Ramaty R., 1992, *ApJ* 389, 739
- Marschhäuser H., 1993, *PhD Thesis*, Ludwig Maximilian Universität, München

- Marschhäuser H., Rieger E., Kanbach G., 1991, Proc. 22nd Int. Cosmic Ray Conf. 2, 463
- Martin, S.F., 1990, Journal of the Italian Astron. Soc., ed. G. Poletto, 61, 293
- Moore R.L., 1990, Journal of the Italian Astron. Soc., ed. G. Poletto, 61, 317
- Murphy R.J., Ramaty R., 1984, Advances in Space Research (Oxford: Pergamon) 4, p. 127
- Murphy R.J., Dermer C.D., Ramaty R., 1987, ApJS 63, 721
- Murphy R.J., et al., 1992, Proc. of the 1st Compton Observatory Symposium, AIP Conf. Proc. 280, 619
- Pick M., 1986, Solar Physics 104, 19
- Ohsawa Y., 1993, Journal of the Phys. Soc. Japan 62, 2382
- Ramaty R., Kozlovsky B., Lingenfelter R.E., 1979, ApJS 40, 487
- Ramaty R., 1986, in: Sturrock, P.A. (ed.) Physics of the Sun, Vol. 2, Nuclear Processes in Solar Flares (Dordrecht: Reidel), p. 291
- Ramaty R., Murphy R.J., Dermer C.D., 1986, Advances in Space Research 6 (Oxford: Pergamon), p. 119
- Ramaty R., Murphy R.J., Dermer C.D., 1987, ApJ 316, L41
- Ramaty R., Miller J.A., Hua X.-M., Lingenfelter R.E., 1990, ApJS 73, 199
- Raoult A., Pick M., Dennis B.R., Kane, S.R., 1985, ApJ 299, 1027
- Rieger E., 1994, ApJS 90, 465
- Rieger E., Marschhäuser H., 1990, in: Winglee R.M., Kiplinger A.L. (eds.) Proceedings Max 91 Workshop (#3) p. 68
- Ryan J.M., Lee M.A., 1991, ApJ 368, 316
- The Radioheliograph Group, 1983, Solar Physics 88, 383
- Trottet G., 1986, Solar Physics 104, 145
- Trottet G., Vilmer N., Barat C., et al., 1993, Adv in Space Res. 13, 205
- Urbaz H.W., 1993 (private communication)
- Wild J.P., Smerd S.F., Weiss A.A., 1963, ARA&A 1, 291
- Wild J.P., Smerd S.F., 1972, Ann. Rev. of Astron. and Astrophys. 10, 159
- Willson R.F., Klein K.-L., Kerdraon A., et al., 1990, ApJ 357, 662
- Willson R.F., 1993, ApJ 413, 798
- Wülser J.P., Canfield R.C., Rieger E., 1990, in: Winglee R.M., Kiplinger A.L. (eds.) Proc. of Max 91 Workshop No. 3 (University of Colorado: Boulder), p. 149

